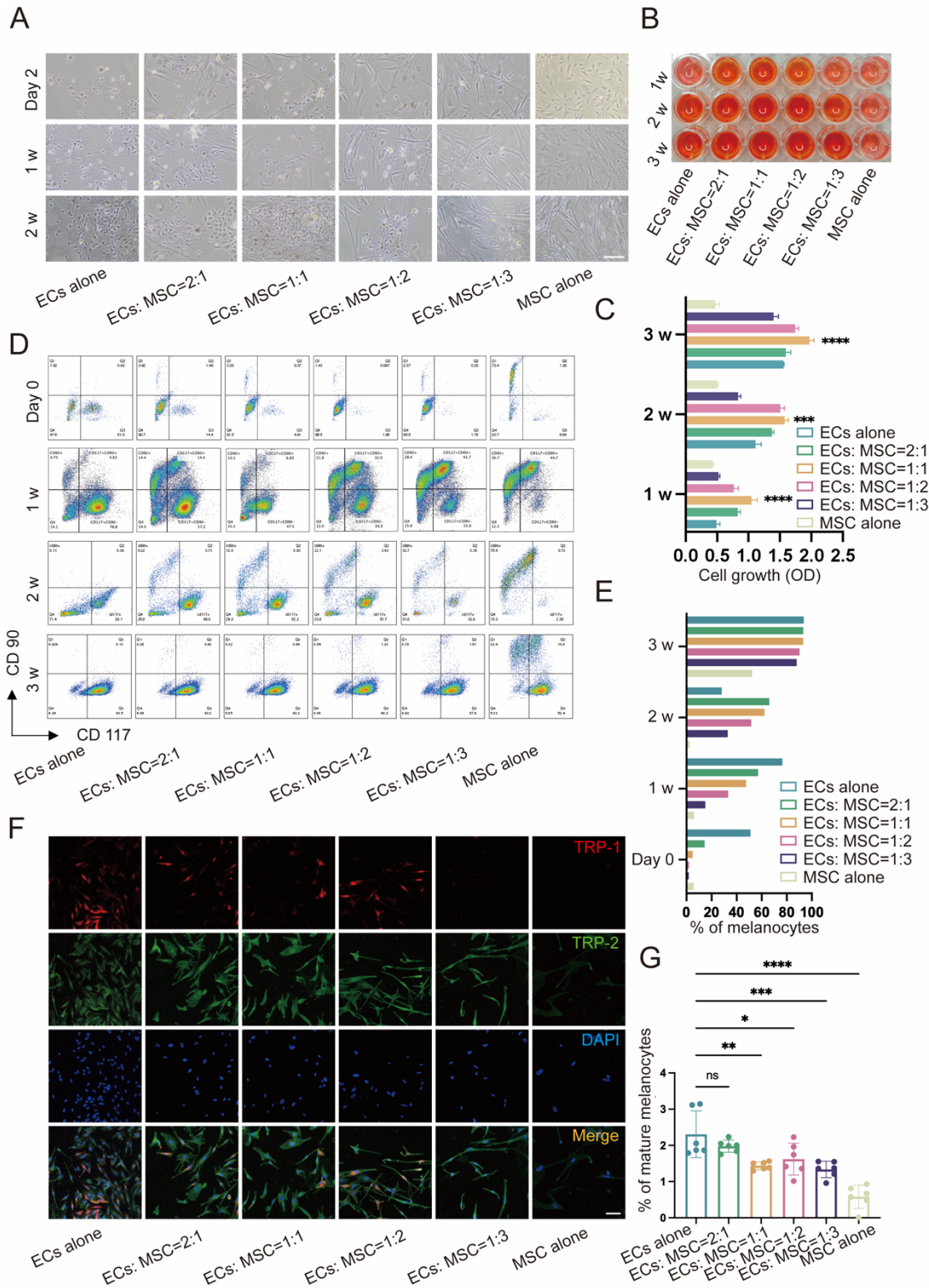


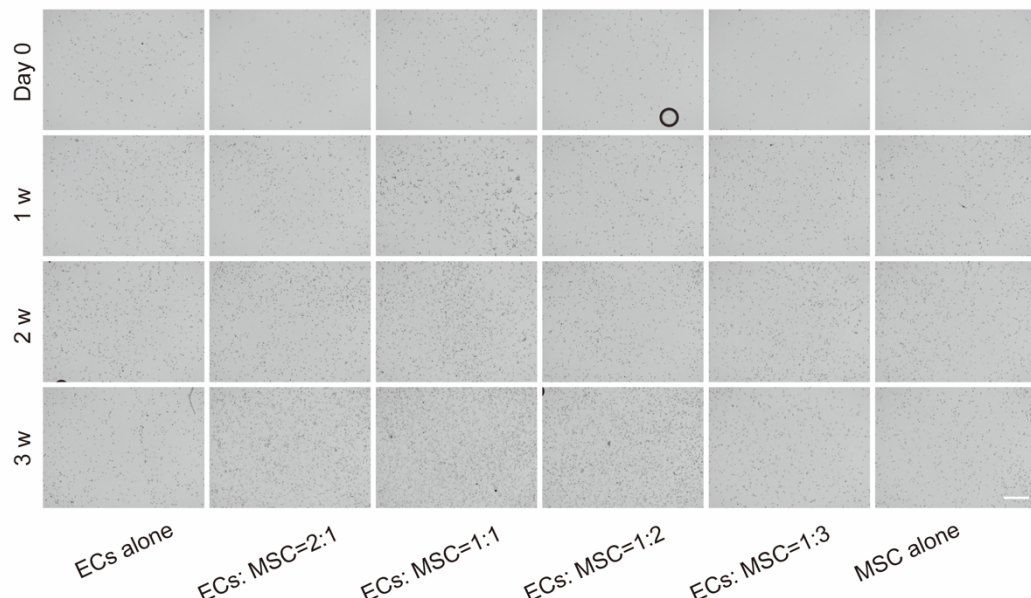
1 **SUPPLEMENTARY MATERIALS**



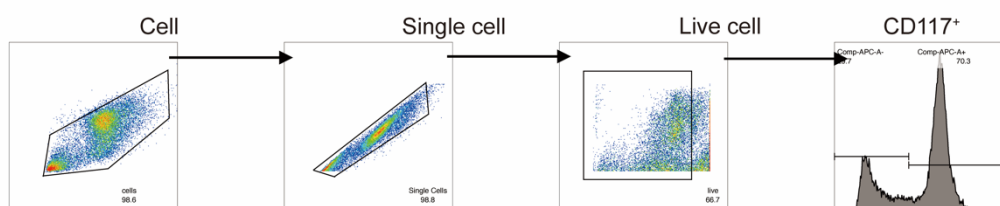
2 **Figure S1. Proliferation and differentiation of ECs co-cultured with hUCMSCs at different ratios.** (A) Observed the proliferation of ECs at different time points by light microscope. Scale bars: 100 μ m. (B) Proliferative ability of ECs of co-culturing with hUCMSCs at different ratio by CCK-8. (C) Quantitative analysis of the proliferation of ECs. (D) Flow cytometry analyzed the percentage of MCs in the co-culture system. (E)

8 Immunofluorescent staining of MCs co-cultured with hUCMScs at different ratios for
9 2 weeks suggested the differentiation situation of MCs. Scale bars: 30 μ m. Data show
10 mean \pm S.D, *P \leq 0.05, **P \leq 0.01, ***P \leq 0.001, ****P \leq 0.0001.

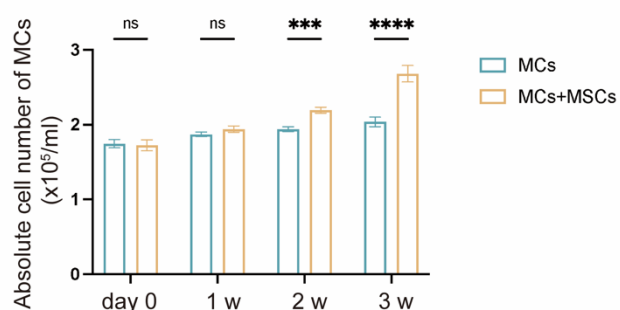
A



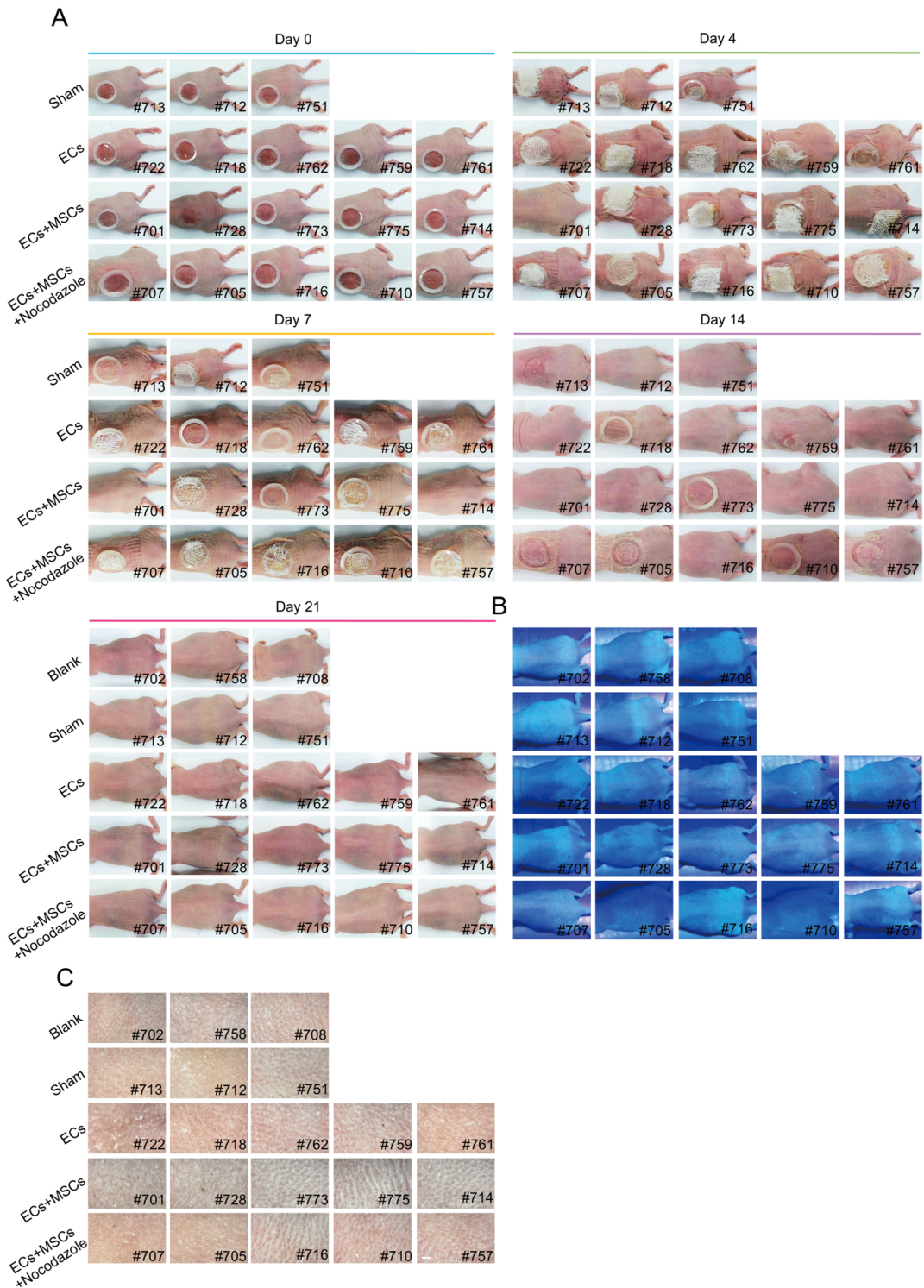
B



C

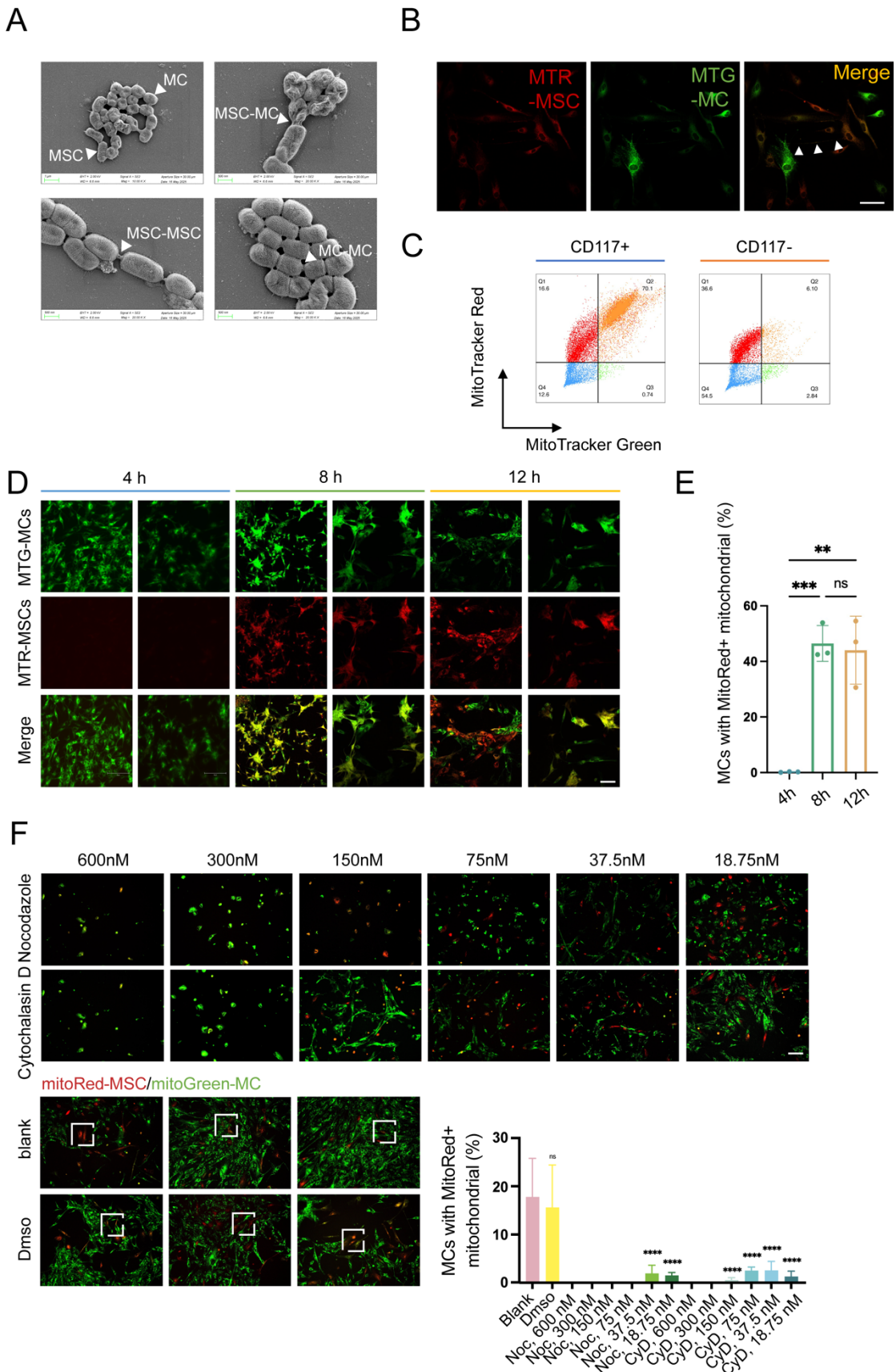


11
12 **Figure S2. The proliferation of MCs in ECs alone and co-culture with hUCMScs.**
13 (A) Cell count on ECs and co-cultured ECs with hUCMScs at different time points.
14 Scale bars: 200 μ m. (B) Gating strategy of CD117 $^{+}$ marked MCs after co-culture by
15 flow cytometry. (C) The absolute cell number of MCs calculated with cell count and
16 flow cytometry. Data show mean \pm S.D, and each experiment was conducted with a
17 minimum of three replicates. ***P \leq 0.001, ****P \leq 0.0001, ns indicates no significant
18 difference by two-way ANOVA.



19

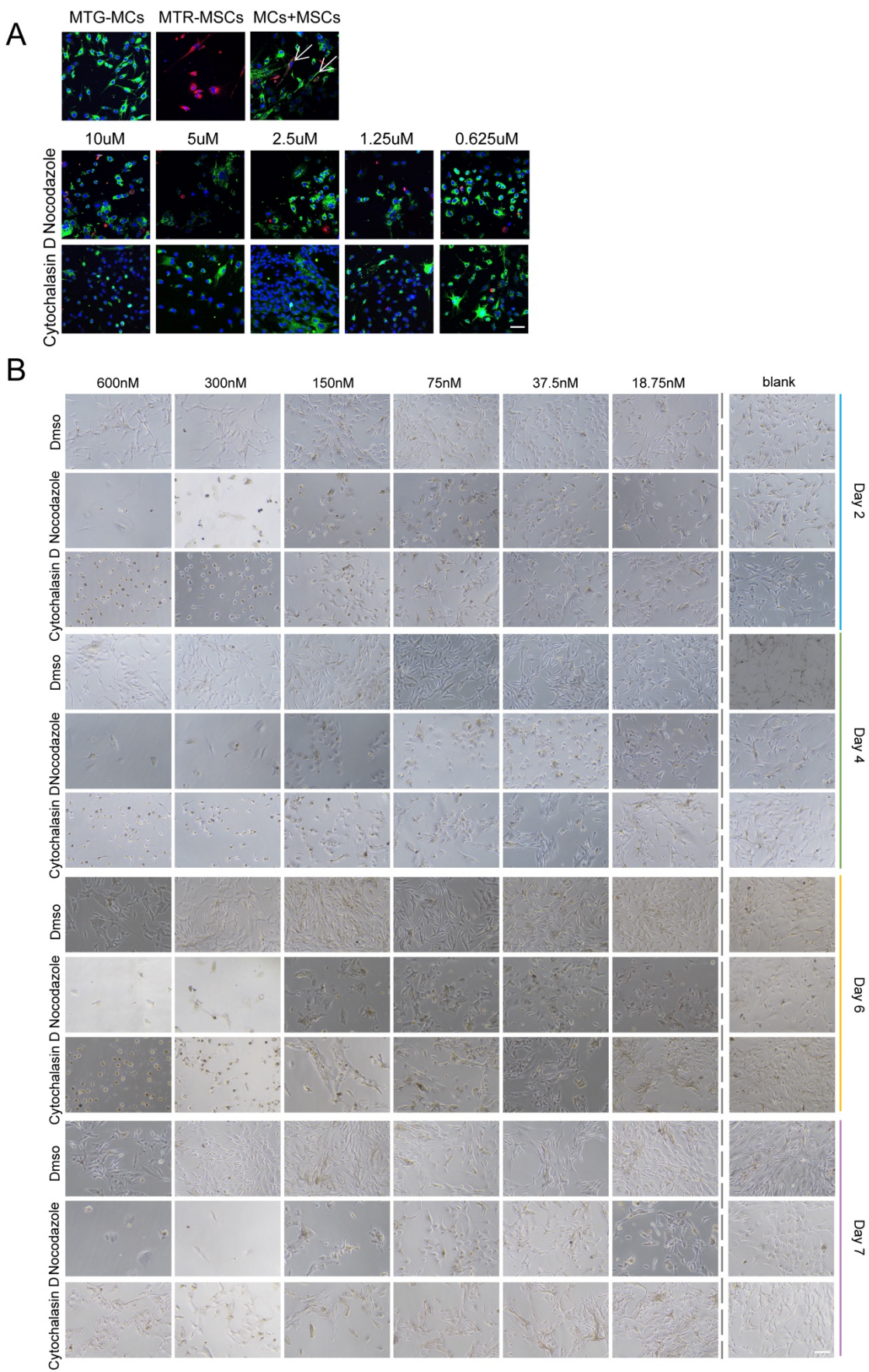
20 **Figure S3. Skin growth and repigmentation on the dorsal side of mice at different**
21 **time points after transplantation. (A)** Observed the repigmentation condition of mice
22 at different time points. **(B)** Wood light analyzed the repigmentation condition of
23 transplantation sites. **(C)** Skin microscope observed the pigmentation at the
24 transplantation sites. Scale bars: 500 μ m.



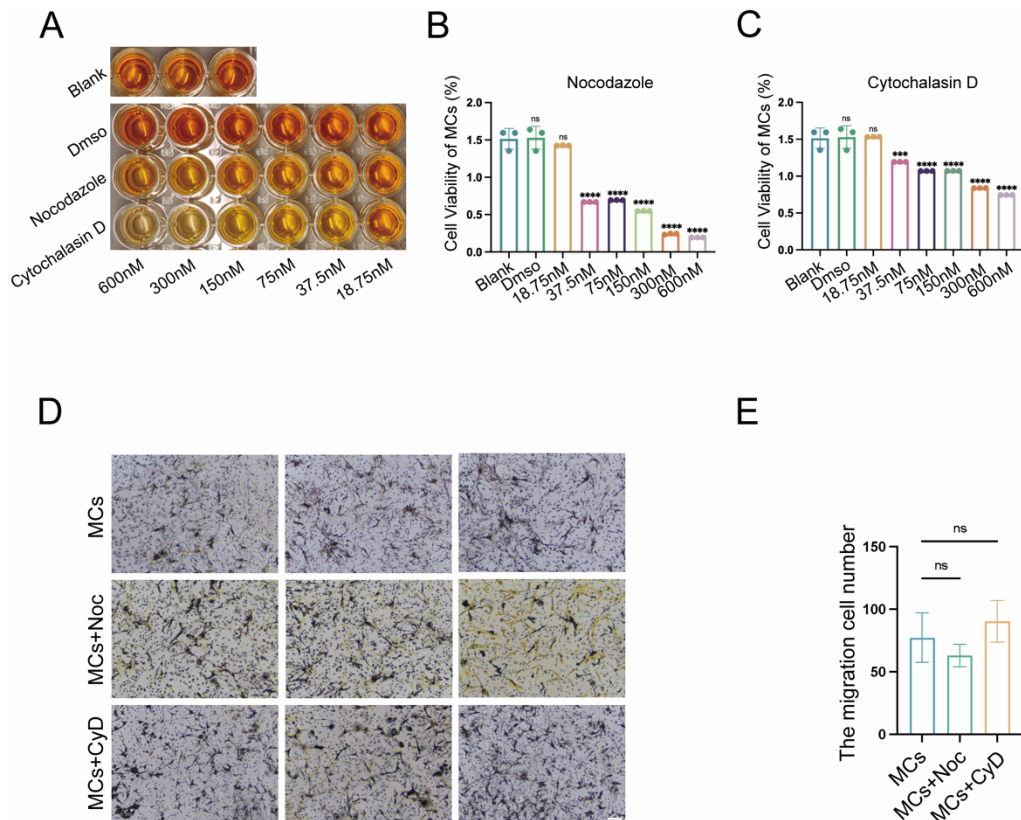
25

26 **Figure S4. Observation of TNTs and selection of blocker concentrations. (A)**
27 **Observation of three types of TNTs by SEM: MSC-MC, MSC-MSC and MC-MC. (B)**

28 Observation of the coexistence of MTG and MTR in the same TNT between MC and
29 MSC using confocal microscopy. Scale bars: 30 μ m. **(C)** Flow cytometry detected the
30 ratio of MTR and MTG in CD117+and CD117- cells. **(D)** Immunofluorescent staining
31 revealed the transfer of mitochondria between the two cells using MTR-hUCMSCs and
32 MTG-MCs at different time points. Scale bars: 30 μ m. **(E)** Statistically analysis of MCs
33 with MTR. **(F)** Immunofluorescent staining observed the blocking status of
34 mitochondrial transfer following treatment with different drug concentrations of Noc
35 or CyD for 7 days. Scale bars: 30 μ m. Data show mean \pm S.D, ** $P \leq 0.01$, *** $P \leq 0.001$,
36 ns indicates no significant difference.



38 **Figure S5. Proliferation of MCs treated with different concentrations of TNT
39 inhibitor.** (A) Immunofluorescent staining observed mitochondrial transfer following
40 treatment with different drug concentrations of Nocodazole (Noc) or Cytochalasin D
41 (CyD) for 8 hours. Scale bars: 30 μ m. (B) Light microscope revealed the proliferation
42 of ECs following treatment with different drug concentrations of Noc or CyD at
43 different time points. Scale bars: 100 μ m.



44
45 **Figure S6. Proliferation and migration of MCs treated with 18.75 nM TNT
46 inhibitor.** (A-C) CCK8 revealed the proliferation of ECs following treatment with
47 different drug concentrations of Noc or CyD at different time points. (D) Migration
48 ability of MC compared with 18.75 nM Nocodazole or Cytochalasin D treated MCs at
49 72 h. Scale bars: 100 μ m. (E) Statistically analysis of migration cell number. Data show
50 mean \pm S.D., ***P \leq 0.001, ****P \leq 0.0001, ns indicates no significant difference.